J.Serb.Chem.Soc. 65(9)661-670(2000)
JSCS-2789

UDC 546.47:543.251:532.517.6
Original scientific paper

Zinc electrodeposition from alkaline zincate solution by pulsating overpotentials

MILOŠ V. SIMIČIĆ[a] and KONSTANTIN I. POPOV[b#]

[a]*Chemical Power Sources Institute, Batajnički put 23, YU-11080 Belgrade (E-mail: IHIS@eunet.yu) and* [b]*Faculty of Technology and Metallurgy, University of Belgrade, Karnegijeva 4, YU-11000 Belgrade, Yugoslavia*

(Received 22 December 1999, revised 26 April 2000)

It is well known that smooth zinc deposits cannot be obtained from alkaline zincate using constant overpotential and current rate. During prolonged metal deposition, spongy and dendritic deposits are formed. It has been shown that the deposits are less agglomerated in the case of square-wave pulsating overpotentials regime than the ones obtained in case of constant overpotential regime. This is explained in a semiquantitative way by two phenomena: selective anodic dissolution during overpotentials "off" period and decreasing diffusion control. These effects is more pronounced at higher pause-to-pulse ratio. Increasing the pause-to-pulse ratio causes a reduction of the ratio between diffusion and activation overpotential, resulting in a more compact deposit. Confirmation of the proposed semiquantitative mathematical model was obtained by zinc electrodeposition onto a copper wire from a 0.1 M zincate solution in 1.0 M KOH at room temperature.

Keywords: zinc electrodeposition, zincate solution, pulsating overpotential, scanning electron microscopy.

INTRODUCTION

It is well known that smooth zinc deposits cannot in fact be obtained from alkaline zincate solutions at constant overpotentials.[1,2] There are three distinct types of zinc deposits reported in the literature.[2–5] At low overpotentials, a mossy deposit is obtained, while at higher overpotentials, near the limiting current, a boulder type of deposit is formed and upon further deposition the boulders preferentially grow into dendrites.

However, smooth deposits can be obtained by using pulsating current,[6] reversing current[7] and pulsating overpotential electrodeposition.[8] It has been reported that the optimum frequency range in electrodeposition at periodically charging rate is 10–100 Hz.[9]

Zinc electrodes in alkaline solution are very studied, mainly because this metal is widely used in electrochemical power sources. However, a short cycle life caused by its disperse deposit, limits its applicability in this field.

Serbian Shemical Society active member.

The purpose of this work was to show the advantage of pulsating overpotential for the elimination of agglomerates and dendrites during zinc deposition. This effect is explained in a semiquantitive way by discussing selective anodic dissolution during the pulsating overpotential "off" period and the reduction of the diffusion control of the deposition process.

EXPERIMENTAL

The electrolyte used throughout this work was a 0.1 mol dm^{-3} zincate solution in 1 mol dm^{-3} KOH. The solution was prepared from AR-grade reagents and tripledistilled water. A concentrated zincate stock solution was made by dissolving ZnO in concentrated CO_2-free KOH solution at 80 to 90 ºC in a flask under reflux in a nitrogen atmosphere. After dilution, the solution was analysed for zinc by EDTA-titration and for KOH by acidimetric titration. All experiments were carried out in a three compartment glass cell at 25.0±0.1 ºC with a tube for bubbling nitrogen.

Zinc was deposited onto a stationary vertical copper cathode. Prior to each experiment, the surface of the electrode was mechanically polished with silicon carbide paper (grits 180, 320 and 600) and then with alumina powders (1.0 and 0.3 μm) and etched in 80 % H_2SO_4 solution. The counter electrode was a high purity (99.99 %) zinc plate and the reference one was a Hg/HgO electrode connected to a Luggin capilary *via* a salt bridge of the test solution.

The experiments with constant polarisation electrolysis consisted of setting the electrode at a constant potential, negative to the rest potential of zinc by means of a PAR-173-potentiostat, for a chosen period of time. A PAR-276-programmer was employed to apply the square pulsating polarisation. The rest potential of zinc in this solution is a mixed potential set up by the zinc dissolution and hydrogen evolution like corrosion couple. Since the corrosion current is small, below 1 μA cm^{-2} and the exchange current density of the zinc dissolution is high, this rest potential will differ only slightly, less than 1 mV, from the equilibrium zinc potential.[10] In the further text, the term overpotential will be used instead of polarisation in the aim of simplicity. After a period of deposition, the electrode was taken out of the cell, washed and dried. The morphologies of the deposits were investigated using a JEOL JSM-35 TEX scanning electron microscopy.

RESULTS AND DISCUSSION

Typical deposits obtained during deposition at low direct overpotential are shown in Fig. 1. The spherical agglomerates of filaments that form spongy deposits was obtained at the applied low overpotentials.

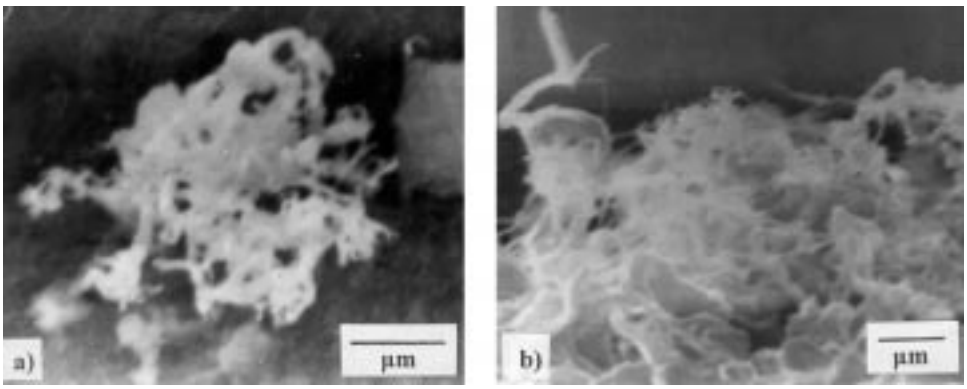

Fig. 1. Zinc deposits at 30 mV a) 25 min, 15000x; b) 25 min, 10000x.

Separate growing zinc boulders were formed at an overpotential η = 90 mV, during electrochemical zinc deposition from 0.1 M K_2ZnO_2 in 1 M KOH. After 20 min deposition, the growth of single sponge agglomerates starts at the steps of these separate growing boulders with hexagonal crystal lattice at the points where they touch each other, *i.e.,* at the points where boulders come into intimate contact, Fig. 2.

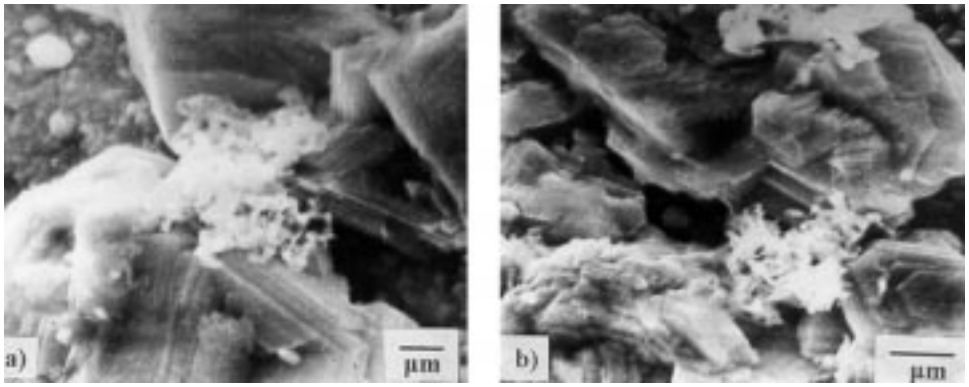

Fig. 2. Zinc deposits at 90 mV a) 20 min, 6600x; b) 20 min, 10000x.

The formation of needles occurred at an overpotential of 220 mV, when spherical diffusion control can be established only around the tips of growing grains, Fig. 3. The growth of needles is possible only if a critical radius has been reached before overlapping of the growing grains begins.[11]

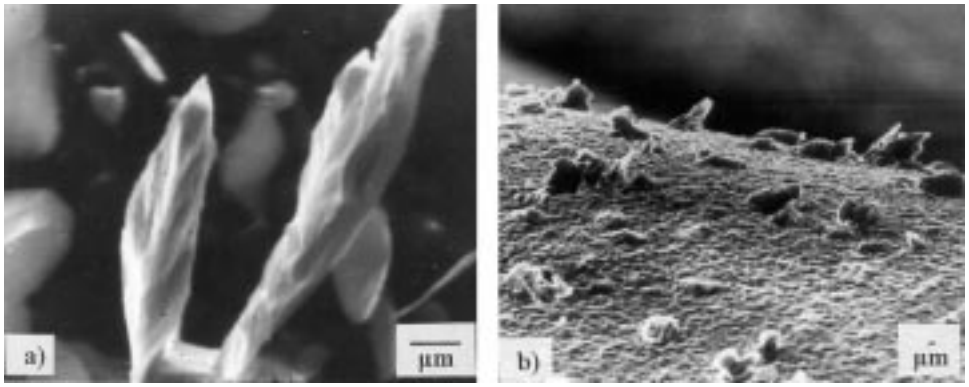

Fig. 3. Zinc deposits at 220 mV a) 3 min, 7500x; b) 7 min, 500x.

At a lower overpotential, η = 130 mV, overlapping of the growing grains occurs and diffusion to the macroelectrode becomes the rate determine step. Then, deposition to the grain will be controlled by linear diffusion and dendritic growth will be initiated,[12] Fig. 4.

Tipycal deposits obtained using a square wave pulsating overpotential are shown in Figs. 5–8.

It is obvious that the deposits become less disperse and less agglomerated with increasing "off" period. The following analyse will explain this phenomena. It

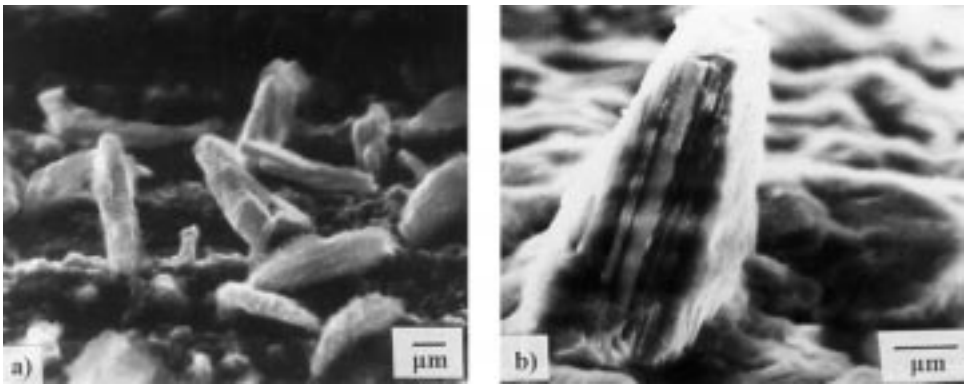

Fig. 4. Zinc deposits at 130 mV a) 6 min, 5000x; b) 7 min, 10000x.

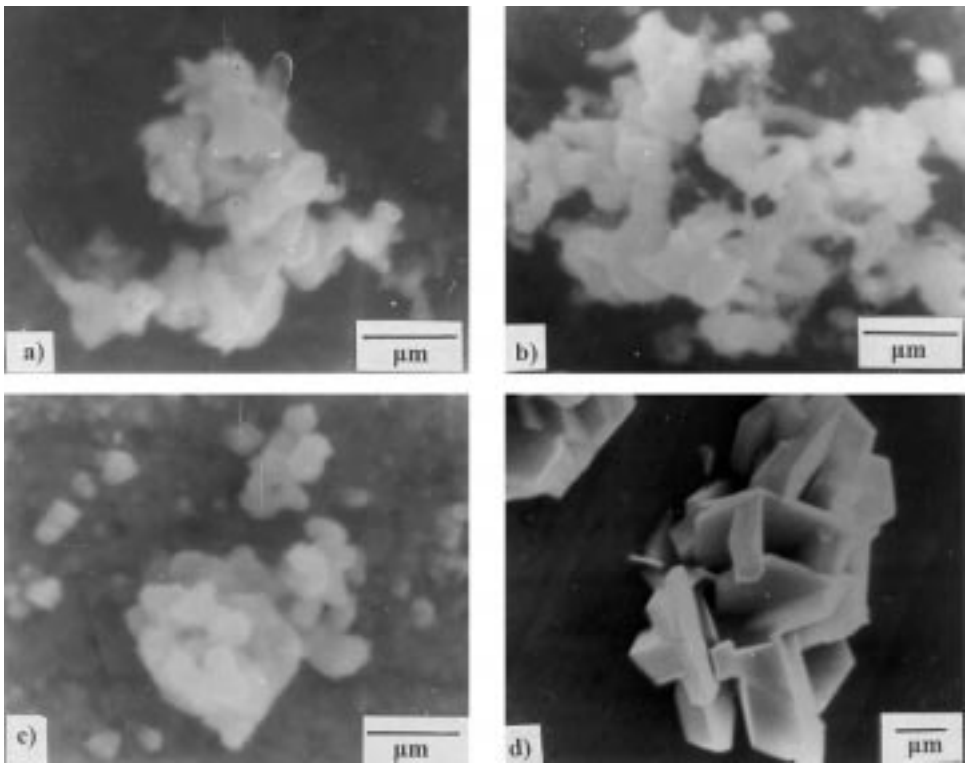

Fig. 5. Zinc deposits at η = 30 mV, ν = 100 Hz. a) p = 1, τ = 1.5 h, 15000x; b) p = 1, τ = 3.0 h, 15000x; c) p = 3, τ = 1.5 h, 15000x; d) p = 9, τ = 5.0 h, 8000x.

is well known that the reversible potential difference between a surface with a radius of curvature, r, and a planar one is:[13]

$$\Delta E = \frac{2\sigma V}{Fr} \tag{1}$$

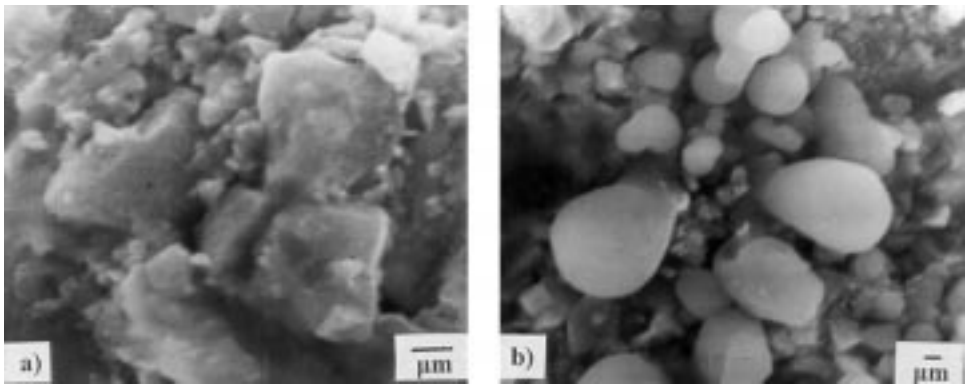

Fig. 6. Zinc deposits at $\eta_{.}$ = 90 mV, ν = 100 Hz. a) p = 1, τ = 25 min, 6400x; b) p = 3, τ = 30 min, 2300x.

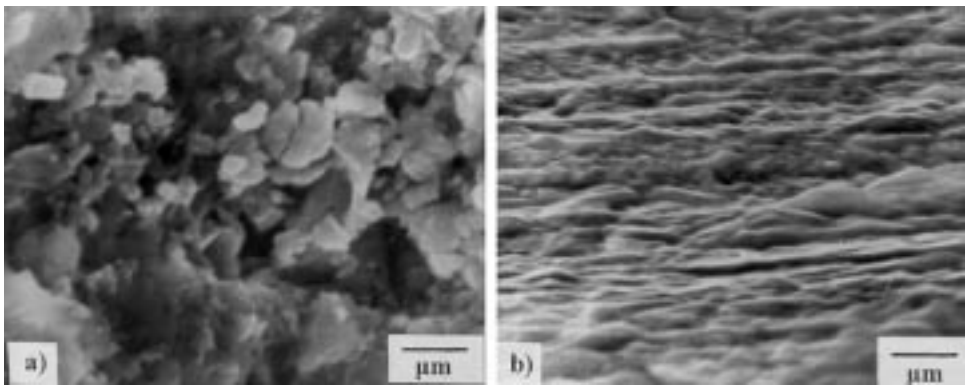

Fig. 7. Zinc deposits at η_A = 130 mV, ν = 100 Hz. a) p = 1, τ = 10 min, 10000x; b) p = 9, τ = 35 min, 10000x.

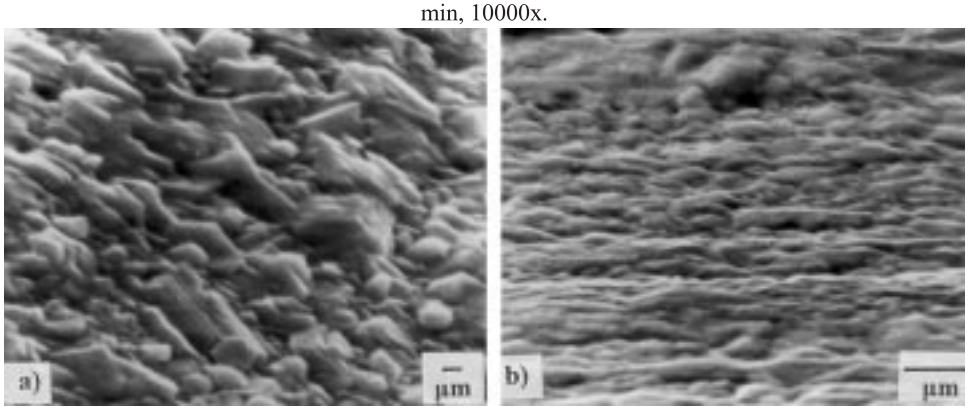

Fig. 8. Zinc deposits at $\eta_{.}$ = 220 mV, ν = 100 Hz. a) p = 3, τ = 20 min, 2500x; b) p = 9, τ = 35 min, 10000x.

This makes the equilibrium potential of spongy zinc deposits from 7 to 10 mV more cathodic than that of zinc foil.[14–16] During the pauses, the tips of curvatures characterized by small radii dissolve faster than the flat surface. In the case of a

square-wave pulsating overpotential, this effect can be quantitatively discussed:

A square-wave pulsating overpotential is defined by:[17]

$$\frac{\partial c}{\partial t} = D\frac{\partial^2 c}{\partial x^2} \tag{2}$$

and

$$c(x,0) = c_0 \tag{3}$$

$$c(\delta, t) = c_0 \tag{4}$$

$$\frac{\partial c(0,t)}{\partial x} = \frac{j_0}{zFD}\left[\frac{c(0,t)}{c_0}\exp\left(\frac{\eta}{\eta_{0,c}}\right) - \exp\left(-\frac{\eta}{\eta_{0,a}}\right)\right] \tag{5}$$

The surface concentration in pulsating overpotential electrodeposition does not vary with time at sufficiently high frequencies and

$$\frac{c(0,t)}{c_0} = 1 - \frac{j_{av}}{j_L} \tag{6}$$

is valid.[17] Substitution of $c(0,t)/c_0$ from Eq. (6) in Eq. (5) gives

$$\frac{\partial c(0,t)}{\partial x} = \frac{j_0}{zFD}\left[\left(1 - \frac{j_{av}}{j_L}\right)\exp\left(\frac{\eta}{\eta_{0,c}}\right) - \exp\left(-\frac{\eta}{\eta_{0,a}}\right)\right] \tag{7}$$

where

$$\eta = \begin{cases} \eta_a \text{ for } mT_p < t \le \left(m + \dfrac{1}{p+1}\right)T_p \\ 0 \text{ for } \left(m + \dfrac{1}{p+1}\right)T_p < t \le (m+1)T_p \end{cases} \tag{8}$$

$m = 0, 1, 2, ...$

Assuming that the surface concentration in pulsating overpotential deposition does not vary with time, it is easy to show that the current response to the input overpotential at sufficiently high frequencies is given by:[9]

$$j = zFD\frac{\partial c(0,t)}{\partial x} =$$

$$= \begin{cases} j_0\left(1 - \dfrac{j_{av}}{j_L}\right)\exp\left(\dfrac{\eta_A}{\eta_{0,c}}\right) - j_0\exp\left(-\dfrac{\eta_A}{\eta_{0,a}}\right) \quad \text{for} \quad mT_p < t \le \left(m + \dfrac{1}{p+1}\right)T_p & \text{(a)} \\ -j_{av}\dfrac{j_0}{j_L} \quad \text{for} \quad \left(m + \dfrac{1}{p+1}\right)T_p < t \le (m+1)T_p & \text{(b)} \end{cases} \tag{9}$$

Equations (2–9) are valid for flat electrode surfaces or protrusions with sufficiently large tip radii, when the surface energy term[13] can be neglected. If it cannot be neglected, the surface energy term affects the reaction rate[18] as defined by Eq. (10)

$$\frac{\partial c(0,t)}{\partial x} = \frac{j_0}{zFD}\left[\left(1-\frac{j_{av}}{j_L}\right)\exp\left(\frac{\eta}{\eta_{0,c}}\right) - \exp\left(\frac{2\sigma V}{RTr}\right)\exp\left(-\frac{\eta}{\eta_{0,a}}\right)\right] \tag{10}$$

The right-hand side of Eq. (7) can be transformed by taking Eq. (10) into account. The output current during pauses ($\eta = 0$) becomes:

$$j = j_0\left(1-\frac{j_{av}}{j_L}\right) - j_0\exp\left(\frac{2\sigma V}{RTr}\right) \tag{11}$$

The difference between the current density at the tip of the irregularities and the flat surface during the "off" period, if $j_{av} \approx j_L$, which is satisfied in most cases of growth of irregularities, is given by:

$$\Delta j = j_0 - j_0\exp\left(\frac{2\sigma V}{RTr}\right) \tag{12}$$

The change of the height of surface protrusions with tip radius r, relative to the flat surface is then given by:[17]

$$\frac{\mathrm{d}h}{\mathrm{d}t} = \Delta j\,\frac{V}{zF} \tag{13}$$

and, finally,

$$h = h_0 + \frac{Vj_0}{zF}\left[1-\exp\left(\frac{2\sigma V}{RTr}\right)\right]t \tag{14}$$

where

$$\left(m+\frac{1}{p+1}\right)T_p < t \le (m+1)T_p \tag{15}$$

Eq. (14) presents the height of the irregularities with tip radius r as a function of time, relative to the flat surface, or to protrusions with sufficiently large r. It is obvious that irregularities with very low tip radii can be completely dissolved during the off-period. This means that branching of irregularities can be prevented in square-wave pulsating overpotential deposition. Obviously, the larger the value of p, the greater the degree of dissolution, as follows from Eq. (14). This effect is more pronounced if η_A remains constant and p increases, as shown in Figs. 5–8.

From another point of view, the effects of pulsating overpotential on the prevention of disperse deposits can be explained in following way.

The average current density during pulsating overpotential deposition can be obtained from[17]

$$j_{\mathrm{av}} = \frac{j_0}{p+1}\left[\left(1-\frac{j_{\mathrm{av}}}{j_{\mathrm{L}}}\right)\exp\left(\frac{\eta_{\mathrm{A}}}{\eta_{0,\mathrm{c}}}\right) - p\,\frac{j_{\mathrm{av}}}{j_{\mathrm{L}}}\right] \tag{16}$$

If the anodic current density is neglected during overpotential pulses, the overpotential amplitude is then given by:

$$\eta_{\mathrm{A}} = \eta_{0,\mathrm{c}}\,\ln\frac{j_{\mathrm{av}}}{j_0} + \eta_{0,\mathrm{c}}\,\ln\left(p+1+\frac{pj_0}{j_{\mathrm{L}}}\right) + \eta_{0,\mathrm{c}}\,\ln\left(\frac{1}{1-\frac{j_{\mathrm{av}}}{j_{\mathrm{L}}}}\right) \tag{17}$$

The third term in Eq. (17) corresponds to bulk diffusion control. It remains constant for a determined average current density regardless of the pause-to-pulse ratio, whereas the second term, which with the first one presents the activation part of the overpotential, increases with increasing p. In this way the ratio, ω, between the overpotential corresponding to bulk diffusion control and the activation overpotential (if $j_{\mathrm{av}} \neq j_{\mathrm{L}}$):

$$\omega = \frac{\ln\dfrac{1}{1-\dfrac{j_{\mathrm{av}}}{j_{\mathrm{L}}}}}{\ln\dfrac{j_{\mathrm{av}}}{j_0} + \ln\left(p+1+\dfrac{pj_0}{j_{\mathrm{L}}}\right)} \tag{18}$$

can be reduced, which leads to the formation of less disperse deposits.

The above discussion and experimental confirmation show that the filaments and the growing grains can be dissolved completely if the pause to pulse ratio is sufficiently high.

This is in accordance with the fact that surfaces with small tip radii have a more negative reversible potential than flat surfaces, which leads to the selective dissolution of deposits during the pauses. Those deposits obtained by pulsating overpotential are more compact compared to deposits obtained at constant overpotential regime, because the activation part of the overpotential is increased compared with the overpotential corresponding to bulk diffusion control in the total overpotential, and the average current density is decreased.

NOMENCLATURE

c concentration
c_0 bulk concentration
D diffusion coefficient
F Faraday constant
h height of a protrusion
h_0 initial height of a protrusion

j current density
j_0 exchange current density
j_{av} average current density
j_L limiting current density
m integer
p pause-to-pulse ratio
R gas constant
r tip radius of a protrusion
T temperature
T_p period
t time
V molar volume
x coordinate in the horizontal direction
z number of electrons
σ surface energy
δ thickness of the diffusion layer
η overpotential
η_A amplitude overpotential
$2.3\eta_{0,c}$ slope of the cathodic Tafel line
$2.3\eta_{0,a}$ slope of the anodic Tafel line

ИЗВОД

ТАЛОЖЕЊЕ ЦИНКА ПУЛСИРАЈУЋИМ ПРЕНАПЕТОСТИМА ИЗ ЦИНКАТНИХ РАСТВОРА

МИЛОШ В. СИМИЧИЋ[а] и КОНСТАНТИН И. ПОПОВ[б]

[а]*Институт за хемијске изворе струје, Батајнички пут 23, 11080 Београд и* [б]*Технолошко-металуршки факултет, Карнегијева 4, 11000 Београд*

Познато је да се глатки талози цинка не могу добити применом константне пренапетости или константне струје. При продуженом таложењу настају сунђерасти или дендритични талози. Показано је да се применом правоугаоне пулсирајуће пренапетости добијају компактнији талози. Ово је објашњено на семи квантитативан начин преко селективног анодног растварања током трајања паузе и смањењем дифузионе контроле процеса. Овај ефекат је више изражен при већим односима трајања паузе према трајању пулса. Повећање односа трајања паузе према трајању пулса смањује утицај дифузионе пренапетости у укупној пренапетости, при чему настају компактнији талози. Потврда предложеног математичког модела показана је при таложењу цинка на бакарну електроду из раствора цинката на собној температури.

(Примљено 22. децембра 1999, ревидирано 26 априла 2000)

REFERENCES

1. K. I. Popov, D. N. Keča, M. D. Anđelić, *J. Appl. Electrochem.* **9** (1978) 19
2. A. R. Despić, J. Diggle, J. O'Bockris, *J. Electrochem. Soc.* **116** (1969) 1503

3. R. D. Naybour, *J. Electrochem. Soc.* **116** (1969) 520
4. J. O'Bockris, Z. Nagy, D. Dražić, *J. Electrochem. Soc.* **120** (1973) 30
5. F. Mansfield, S. Gilman, *J. Electrochem. Soc.* **117** (1970) 1520
6. V. V. Romanov, *Zh. Prikl. Khim.* **36** (1963) 1057
7. S. Arouete, K. F. Blurton, H. G. Oswin, *J. Elekctrochem. Soc.* **116** (1969) 166
8. A. R. Despić, K. I. Popov, *J. Appl. Electrochem.* **1** (1971) 275
9. K. I. Popov, M. G. Pavlović, "Electrodeposition of metal powders with controlled particle grain size and morphology" in *Modern Aspects of Electrochemistry, Vol XXIV,* R. E. White *et al.,* Eds., Plenum Press, New York, 1993, p. 299
10. J. O'M. Bockris, Z. Nagy, A. Damjanović, *J. Electrochem. Soc.* **119** (1972) 285
11. K. I. Popov, N. V. Krstajić, S. R. Popov, *J. Appl. Electrochem.* **15** (1985) 151
12. A. R. Despić, K. I. Popov, "Transport controlled deposition and dissolution of metal" in *Modern Aspects of Electrochemistry, Vol. VII,* B. E. Conway and J. O'M. Bockris, Eds., Plenum Press, New York, 1972, p. 199
13. J. L. Barton, J. O'Bockris, *Proc. Roy. Soc., London* **A268** (1962) 485
14. A. Aroute, K. F. Blurton, H. G. Oswin, *J. Electrochem. Soc.* **116** (1969) 166
15. R. Yu. Bek, N. T. Kudryavtsev, *Zh. Prikl. Khim.* **34** (1961) 2013
16. R. Yu. Bek, N. T. Kudryavtsev, *Zh. Prikl. Khim.* **34** (1961) 2020
17. K. I. Popov, M. D. Masimović, "Theory of the effects of electrodeposition at a periodically changing rate on the morphology of metal deposits" in *Modern Aspects of Electrochemistry, Vol. XIX,* B. E. Conway, J. O'M. Bockris and R. E. White, Eds., Plenum Press, New York, 1989, p. 193
18. K. I. Popov, M. G. Pavlović, B. V. Toperić, *J. Serb. Shem. Soc.* **55** (1990) 671.